Inorganic Chemistry

Article

pubs.acs.org/IC

Models for B_{12}-Conjugated Radiopharmaceuticals. Cobaloxime Binding to New *fac*-[$Re(CO)_3(Me_2Bipyridine)(amidine)]BF_4$ Complexes Having an Exposed Pyridyl Nitrogen

Nerissa A. Lewis, Patricia A. Marzilli, Frank R. Fronczek, and Luigi G. Marzilli*

Department of Chemistry, Louisiana State University, Baton Rouge, Louisiana 70803, United States

Supporting Information

ABSTRACT: New mononuclear amidine complexes, *fac*-[$Re(CO)_3(Me_2bipy)(HNC(CH_3)$-(pyppz))]$BF_4$ [(4,4′-Me_2bipy (**1**), 5,5′-Me_2bipy (**2**), and 6,6′-Me_2bipy (**3**)] (bipy = 2,2′-bipyridine), were synthesized by treating the parent *fac*-[$Re^I(CO)_3(Me_2bipy)(CH_3CN)]BF_4$ complex with the C_2-symmetrical amine 1-(4-pyridyl)piperazine (pyppzH). The axial amidine ligand has an exposed, highly basic pyridyl nitrogen. The reaction of complexes **1**−**3** with a B_{12} model, (py)$Co(DH)_2Cl$ (DH = monoanion of dimethylglyoxime), in CH_2Cl_2 yielded the respective dinuclear complexes, namely, *fac*-[$Re(CO)_3(Me_2bipy)(\mu$-$(HNC(CH_3)(pyppz)))Co$-$(DH)_2Cl]BF_4$ [(4,4′-Me_2bipy (**4**), 5,5′-Me_2bipy (**5**), and 6,6′-Me_2bipy (**6**)]. ^1H NMR spectroscopic analysis of all compounds and single-crystal X-ray crystallographic data for **2**, **3**, **5**, and **6** established that the amidine had only the *E* configuration in both the solid and solution states and that the pyridyl group is bound to Co in **4**−**6**. Comparison of the NMR spectra of **1**−**3** with spectra of **4**−**6** reveals an unusually large "wrong-way" upfield shift for the pyridyl H2/6 signal for **4**−**6**. The wrong-way H2/6 shift of (4-Xpy)$Co(DH)_2Cl$ (4-Xpy = 4-substituted pyridine) complexes increased with increasing basicity of the 4-Xpy derivative, a finding attributed to the influence of the magnetic anisotropy of the cobalt center on the shifts of the ^1H NMR signals of the pyridyl protons closest to Co. Our method of employing a coordinate bond for conjugating the *fac*-[$Re^I(CO)_3$] core to a vitamin B_{12} model could be extended to natural B_{12} derivatives. Because B_{12} compounds are known to accumulate in cancer cells, such an approach is a very attractive method for the development of ^{99m}Tc and $^{186/188}Re$ radiopharmaceuticals for targeted tumor imaging and therapy.

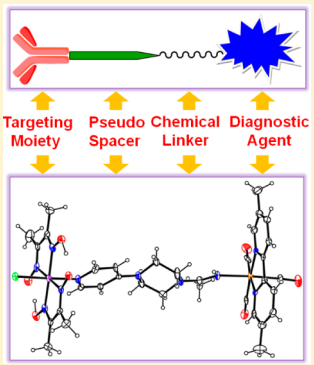

INTRODUCTION

Isotopes of rhenium and technetium are among the most promising nuclides utilized in diagnostic and therapeutic applications.[1−3] Rhenium and technetium complexes bearing the *fac*-[$M^I(CO)_3$] core have received much attention owing to the many ideal properties of this core.[4−7] Some *fac*-[$^{99m}Tc^I(CO)_3L]^n$ imaging agents have recently undergone evaluations in humans,[4,7,8] and *fac*-[$^{186/188}Re^I(CO)_3L]^n$ agents are emerging among the most promising radionuclides for therapeutic applications.[1−4]

The concept of combining ^{99m}Tc and $^{186/188}Re$ with bioactive molecules to produce selective targeting agents is currently receiving much attention.[2−4,9−15] Investigations involving *fac*-[$Re^I(CO)_3L]^n$ complexes prepared with naturally abundant rhenium offer both guidance in the development of new radiopharmaceuticals and deep insight into the chemistry and biomedical characteristics of $^{186/188}Re$ therapeutic agents and ^{99m}Tc diagnostic agents.[1−3,7,10,16−18] We have been exploring the chemistry of complexes containing the *fac*-[$Re^I(CO)_3$] core to broaden the methods for linking [$Re^I(CO)_3L]^n$ complexes to targeting molecules.[4,16,19−21] We focus particularly on developing new chemistry in which the bioconjugation involves a monodentate ligand rather than the multidentate ligands most often used.[15,16,21−24]

We have recently been investigating the monodentate ligands having a superbasic amidine donor group.[4,19] In our first study, we discovered that primary amines added to acetonitrile complexes having bidentate substituted bipyridines, *fac*-[$Re^I(CO)_3(Me_2bipy)(CH_3CN)]BF_4$ (bipy = 2,2′-bipyridine), form robust *fac*-[$Re(CO)_3(Me_2bipy)(HNC(CH_3)NHR)]BF_4$ complexes.[19] Thus, amidine groups have potential as linkers for the conjugation of the *fac*-[$M^I(CO)_3$] core (M = ^{99m}Tc and $^{186/188}Re$ radionuclides) to bioactive targeting moieties.[4,19] The Re^I amidine moiety, Re^I−N3(H)−$C_{am}(CH_3)$−N4(H)R, in these reported complexes has two different substituents (H and R) on the remote nitrogen (N4) and double-bond character in the C−N bonds (C_{am}−N3 and C_{am}−N4).[19] These features lead to the possibility of four configurations and hence four conceivable isomers for *fac*-[$Re(CO)_3(Me_2bipy)$-$(HNC(CH_3)NHR)]BF_4$ complexes (Figure 1).[19] In some solvents, as many as three isomers were found to exist and to undergo interchange, properties limiting the application of such amidines in radiopharmaceutical development. Bulky R groups destabilized the *Z* and *Z*′ configurations.[19]

Recently we overcame the "isomer problem" by forming the amidines by using bulky C_2-symmetrical saturated heterocyclic

Received: July 11, 2014
Published: October 6, 2014

 © 2014 American Chemical Society dx.doi.org/10.1021/ic5016675 | *Inorg. Chem.* 2014, 53, 11096−11107

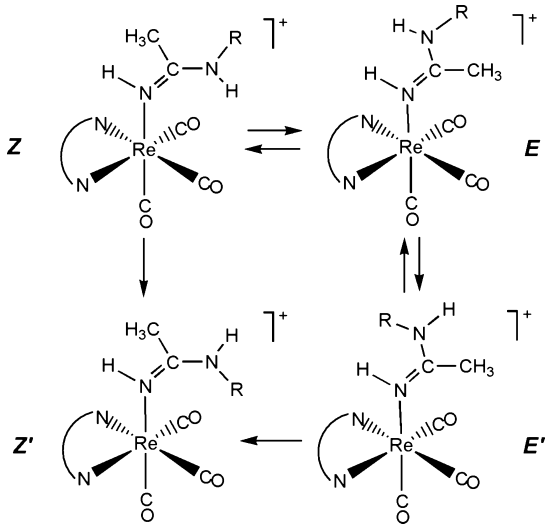

Figure 1. All conceivable isomers of mononuclear *fac*-[Re(CO)$_3$(Me$_2$bipy)(HNC(CH$_3$)(NHR))]BF$_4$ complexes, in which bidentate ligands (4,4′-Me$_2$bipy, 5,5′-Me$_2$bipy, or 6,6′-Me$_2$bipy) are denoted by the two N donor atoms connected by a curved line.

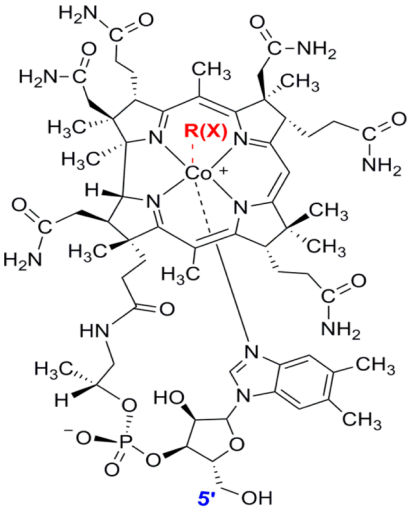

Figure 2. Schematic structural representation of the cobalamins (Cbl): cyanocobalamin (X = CN, vitamin B$_{12}$, CNCbl), methylcobalamin (R = CH$_3$, MeCbl), and coenzyme B$_{12}$ (R = 5′-deoxy-5′-adenosyl, adenosylcobalamin, AdoCbl).

secondary amines (HN(CH$_2$CH$_2$)$_2$Y; Y = CH$_2$, (CH$_2$)$_2$, (CH$_2$)$_3$, NH, or O).[4] Only two configurations (*E* and *Z*) are possible when the two N4 substituents are equal, and the bulk of two CH$_2$CH$_2$ chains attached to N4 was expected to destabilize the *Z* configuration. Complexes of the type *fac*-[Re(CO)$_3$(Me$_2$bipy)(HNC(CH$_3$)N(CH$_2$CH$_2$)$_2$Y)]BF$_4$ (Me$_2$bipy = 5,5′-Me$_2$bipy or 6,6′-Me$_2$bipy)[4] were prepared and found to be robust and to exist as only one isomer having the *E* configuration.[4]

In the present study, we prepare analogues of the *fac*-[Re(CO)$_3$(L)(HNC(CH$_3$)N(CH$_2$CH$_2$)$_2$Y)]BF$_4$ complexes,[4] but with a novel dangling and potentially metal-ligating donor group incorporated with Y. Such donors can coordinate to metal centers with targeting or therapeutic potential, thereby allowing us to use coordinate bonds in the approach to form bioconjugates. We test our approach by using a pendant pyridyl group and B$_{12}$ model compounds. In contrast to healthy body cells, rapidly dividing cells (such as those present at the site of tumors or bacterial infections) have an increased demand for cobalamins (also known as B$_{12}$, Figure 2).[25−35] The use of B$_{12}$ for the targeted delivery of cytotoxic and radiotoxic agents to tumor sites has therefore attracted much attention.[25,28,34,36−38]

Treatment of *fac*-[Re^{I}(CO)$_3$(Me$_2$bipy)(CH$_3$CN)]BF$_4$ complexes with the C_2-symmetrical 1-(4-pyridyl)piperazine (pyppzH) amine afforded new amidine complexes *fac*-[Re(CO)$_3$(Me$_2$bipy)(HNC(CH$_3$)(pyppz))]BF$_4$. As expected, the amidine ligand has only the *E* configuration and contains an exposed pyridyl nitrogen atom available to coordinate to a target metal center. Treatment of the *fac*-[Re(CO)$_3$(Me$_2$bipy)(HNC(CH$_3$)(pyppz))]BF$_4$ complexes with a simple B$_{12}$ model, (py)Co(DH)$_2$Cl (DH = monoanion of dimethylglyoxime), produced dinuclear complexes *fac*-[Re(CO)$_3$(Me$_2$bipy)(μ-(HNC(CH$_3$)(pyppz)))Co(DH)$_2$Cl]BF$_4$, which have a direct coordinate bond between the amidine ligand pyridyl ring N atom and the cobalt atom. Because all of these new complexes exhibit facial geometry, we shall omit the *fac*- designation below when discussing the complexes.

EXPERIMENTAL SECTION

Starting Materials. Re$_2$(CO)$_{10}$, 4,4′-dimethyl-2,2′-bipyridine (4,4′-Me$_2$bipy), 5,5′-dimethyl-2,2′-bipyridine (5,5′-Me$_2$bipy), 6,6′-dimethyl-2,2′-bipyridine (6,6′-Me$_2$bipy), pyridine (py), 4-cyanopyridine (4-CNpy), 4-dimethylaminopyridine (4-Me$_2$Npy), 4-methoxypyridine (4-MeOpy), 4-methylpyridine (4-Mepy), piperazine (ppzH), 1-(4-pyridyl)piperazine (pyppzH), 1-(4-pyridyl)piperidine (4-(CH$_2$)$_5$Npy), and AgBF$_4$ were obtained from Sigma-Aldrich. Known methods were employed to prepare the following: Re(CO)$_5$Br,[39] [Re(CO)$_3$(CH$_3$CN)$_3$]BF$_4$,[20,40] [Re(CO)$_3$(Me$_2$bipy)(CH$_3$CN)]BF$_4$,[19] and (py)Co(DH)$_2$Cl.[41]

NMR Measurements. ^{1}H NMR spectra were recorded on a 400 MHz Bruker spectrometer. Peak positions are relative to tetramethylsilane (TMS) or solvent residual peak, with TMS as reference. All NMR data were processed with TopSpin and Mestre-Nova software. For specific assignments of signals listed in the syntheses described below, please see tables in the text and in Supporting Information.

X-ray Data Collection and Structure Determination. Intensity data were collected at low temperature on a Bruker Kappa Apex-II DUO CCD diffractometer fitted with an Oxford Cryostream cooler and either graphite-monochromated Mo Kα (λ = 0.710 73 Å) radiation or (for **2**) Cu Kα (λ = 1.541 84 Å) radiation from an IμS microfocus source with multilayer optics. Data reduction included absorption corrections by the multiscan method, with SADABS.[42] All X-ray structures were determined by direct methods and difference Fourier techniques and refined by full-matrix least-squares methods by using SHELXL97.[43]

General Synthesis of [Re(CO)$_3$(Me$_2$bipy)(HNC(CH$_3$)(pyppz))]BF$_4$ Complexes. All of the mononuclear amidine complexes (Scheme 1) were synthesized by a slight modification of a known procedure.[4] An acetonitrile solution (6 mL) of a [Re(CO)$_3$(Me$_2$bipy)(CH$_3$CN)]BF$_4$ complex (40 mg, 0.06 mmol) was treated with pyppzH (30 mg, 0.18 mmol); the reaction mixture was stirred at room temperature for 4 h and then reduced in volume to ∼1 mL by rotary evaporation. The addition of diethyl ether to the point of cloudiness (∼5−10 mL) produced a yellow crystalline material that was collected on a filter, washed with diethyl ether, and dried.

*[Re(CO)$_3$(4,4′-Me$_2$bipy)(HNC(CH$_3$)(pyppz))]BF$_4$ (**1**).* The use of the general method in the reaction of [Re(CO)$_3$(4,4′-Me$_2$bipy)(CH$_3$CN)]BF$_4$ with pyppzH afforded 32 mg (50% yield) of yellow crystalline material. For ^{1}H NMR data in CD$_2$Cl$_2$, see Table 1 and Supporting Information. ESI-MS (*m*/*z*): [M + H]$^+$ = 659.1780. Calcd for [M + H]$^+$ = 659.1780.

dx.doi.org/10.1021/ic5016675 | Inorg. Chem. 2014, 53, 11096−11107

Scheme 1. Synthesis of Mononuclear Amidine Complexes, Showing the Numbering Systems for Ligands in the Reaction of $[Re(CO)_3(Me_2bipy)(CH_3CN)]BF_4$ with pyppzH[a]

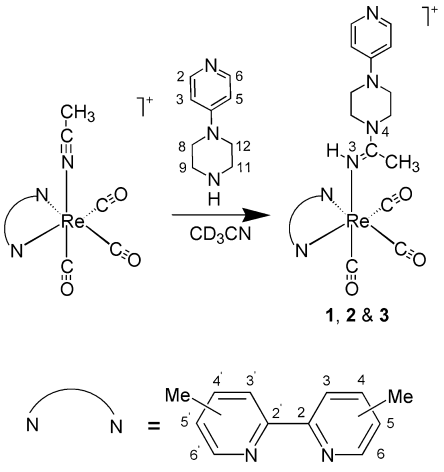

[a]Me_2bipy = 4,4′-, 5,5′-, or 6,6′-Me_2bipy.

*[Re(CO)$_3$(5,5′-Me$_2$bipy)(HNC(CH$_3$)(pyppz))]BF$_4$ (**2**).* The use of the general method in the reaction of $[Re(CO)_3(5,5'\text{-}Me_2bipy)(CH_3CN)]BF_4$ with pyppzH afforded 39 mg (61% yield) of yellow crystalline material. For ^{1}H NMR data in CD_2Cl_2, see Table 1 and Supporting Information. X-ray quality crystals grew from a solution of the crystalline material (10 mg/1 mL of CH_2Cl_2) in a lightly stoppered container after the addition of 8 mL of diethyl ether.

*[Re(CO)$_3$(6,6′-Me$_2$bipy)(HNC(CH$_3$)(pyppz))]BF$_4$ (**3**).* The use of the general method in the reaction of $[Re(CO)_3(6,6'\text{-}Me_2bipy)(CH_3CN)]BF_4$ with pyppzH afforded 33 mg (51% yield) of yellow crystalline material. For ^{1}H NMR data in CD_2Cl_2, see Table 1 and Supporting Information. X-ray quality crystals grew from a solution of the material (10 mg/1 mL of CH_2Cl_2) in a lightly stoppered container after the addition of 10 mL of diethyl ether.

General Synthesis of [Re(CO)$_3$(Me$_2$bipy)(μ-(HNC(CH$_3$)(pyppz)))Co(DH)$_2$Cl]BF$_4$ Dinuclear Complexes. The $[Re(CO)_3(Me_2bipy)(HNC(CH_3)(pyppz))]BF_4$ complex (30 mg, 0.04 mmol) was dissolved in CH_2Cl_2 (6 mL) and treated with $(py)Co(DH)_2Cl$ (16 mg, 0.04 mmol), and the reaction mixture was stirred at room temperature for 24 h. The volume was reduced to ∼1 mL by rotary evaporation. Addition of diethyl ether (∼5−10 mL) to the point of cloudiness produced a yellow crystalline material that was collected on a filter, washed with diethyl ether, and dried.

*[Re(CO)$_3$(4,4′-Me$_2$bipy)(μ-(HNC(CH$_3$)(pyppz))(Co(DH)$_2$Cl]BF$_4$ (**4**).* The use of the general method for the reaction of $[Re(CO)_3(4,4'\text{-}Me_2bipy)(HNC(CH_3)(pyppz))]BF_4$ with $(py)Co(DH)_2Cl$ afforded 21 mg (66% yield) of yellow crystalline material. For ^{1}H NMR data in CD_2Cl_2, see Table 1 and Supporting Information. ESI-MS(m/z): $[M + H]^+$ = 983.1884. Calcd for $[M + H]^+$ = 983.1816.

*[Re(CO)$_3$(5,5′-Me$_2$bipy)(μ-(HNC(CH$_3$)(pyppz)))Co(DH)$_2$Cl]BF$_4$ (**5**).* The use of the general method for the reaction of $[Re(CO)_3(5,5'\text{-}Me_2bipy)(HNC(CH_3)(pyppz))]BF_4$ with $(py)Co(DH)_2Cl$ afforded 24 mg (75% yield) of yellow crystalline material. For ^{1}H NMR data in CD_2Cl_2, see Table 1 and Supporting Information. X-ray quality crystals were obtained from a solution of the material (10 mg/1 mL of CH_2Cl_2) in a lightly stoppered container after the addition of 8 mL of diethyl ether.

*[Re(CO)$_3$(6,6′-Me$_2$bipy)(μ-(HNC(CH$_3$)(pyppz)))Co(DH)$_2$Cl]BF$_4$ (**6**).* The use of the general method for the reaction of $[Re(CO)_3(6,6'\text{-}Me_2bipy)(HNC(CH_3)(pyppz))]BF_4$ with $(py)Co(DH)_2Cl$ afforded 25 mg (78% yield) of yellow crystalline material. For ^{1}H NMR data in CD_2Cl_2, see Table 1 and Supporting Information. X-ray quality crystals were obtained from a solution of the material (10 mg/1 mL of CH_2Cl_2) in a lightly stoppered container after the addition of 10 mL of diethyl ether.

RESULTS AND DISCUSSION

Synthesis. Treatment of $[Re(CO)_3(Me_2bipy)(CH_3CN)]BF_4$ (Me_2bipy = 4,4′-Me_2bipy, 5,5′-Me_2bipy, and 6,6′-Me_2bipy) with pyppzH in acetonitrile at room temperature afforded good yields (usually 50−60%) of new mononuclear amidine complexes, $[Re(CO)_3(Me_2bipy)(HNC(CH_3)(pyppz))]BF_4$ [Me_2bipy = 4,4′-Me_2bipy (**1**), 5,5′-Me_2bipy (**2**), and 6,6′-Me_2bipy (**3**)], as illustrated in Scheme 1.

Numerous similarities in the chemical and physical properties exist between simple pseudo-octahedral cobaloximes $LCo^{III}(DH)_2$(monoanion) [L = neutral ligand, DH = monoanion of dimethylglyoxime, and monoanion = an inorganic (X) or an alkyl (R) ligand] and B_{12}.[44−46] The well-defined relationships between the structural and spectroscopic properties revealed by the study of simple B_{12} model compounds facilitate the interpretation of spectral trends (or

Table 1. ^{1}H NMR Chemical Shifts (ppm) of $[Re(CO)_3(Me_2bipy)(HNC(CH_3)(pyppz))]BF_4$ and $[Re(CO)_3(Me_2bipy)(\mu\text{-}(HNC(CH_3)(pyppz)))Co(DH)_2Cl]BF_4$ Complexes in CD_2Cl_2 at 25 °C

	1	2	3	4	5	6
	4,4′-Me_2bipy	5,5′-Me_2bipy	6,6′-Me_2bipy	4,4′-Me_2bipy	5,5′-Me_2bipy	6,6′-Me_2bipy
N3H	4.70	4.73	5.14	4.69	4.70	5.03
$C_{am}CH_3$	2.37	2.38	1.95	2.33	2.35	1.89
			pyppz signals			
H2/6	8.17	8.18	8.20	7.53	7.54	7.54
H3/5	6.54	6.53	6.54	6.32	6.32	6.35
H8/12	3.34	3.34	3.34	3.32	3.34	3.33
H9/11	3.34	3.34	3.34	3.32	3.34	3.33
			Me_2bipy signals			
H3/3′	8.32	8.33	8.20	8.25	8.27	8.21
H4/4′		8.02	8.06		7.99	8.03
H5/5′	7.41		7.56	7.39		7.54
H6/6′	8.74	8.73		8.71	8.70	
CH_3	2.63	2.51	3.06	2.61	2.49	3.05
			oxime signals			
CH_3				2.31	2.31	2.31
OH···O				18.40	18.39	18.37

dx.doi.org/10.1021/ic5016675 | Inorg. Chem. 2014, 53, 11096−11107

structural data) observed for the larger, more complicated cobalamins.[46−49]

Analytically pure cobaloximes, $LCo^{III}(DH)_2X$, prepared by the usual procedure involving air oxidation,[41] contain traces (<0.1%) of $LCo^{II}(DH)_2$.[50,51] These traces of $LCo^{II}(DH)_2$ catalyze a rapid ligand-exchange reaction (eq 3) that proceeds by the mechanism described by eqs 1−3.[50−53] The time for the reaction depends on the amount of trace Co^{II} present.

$$\text{fast: } LCo^{II}(DH)_2 + L' \leftrightarrow L'Co^{II}(DH)_2 + L \quad (1)$$

$$\text{slow: } LCo^{III}(DH)_2X + L'Co^{II}(DH)_2 \rightarrow L'Co^{III}(DH)_2X + LCo^{II}(DH)_2 \quad (2)$$

$$LCo^{III}(DH)_2X + L' \rightarrow L'Co^{III}(DH)_2X + L \quad (3)$$

The rate-determining step (2) is shown as being irreversible because in past studies as well as in this study, ordinarily L′ is a much better ligand than L. All evidence indicates that step 2 involves an inner-sphere electron-transfer process.[50−52] The activated complex for this step, $LCo^{III}(DH)_2{-}X{-}Co^{II}(DH)_2L'$, has a bridging chloro ligand.[50−52]

We utilized this facile exchange process by treating $(py)Co(DH)_2Cl$ with complexes **1**−**3** (Scheme 2) to produce

Scheme 2. Synthesis of Re,Co Dinuclear Complexes by the Reaction of $[Re(CO)_3(Me_2bipy)(HN(CH_3)_2(pyppz))]BF_4$ (Me_2bipy = 4,4′-, 5,5′-, or 6,6′-Me_2bipy) with $(py)Co(DH)_2Cl$

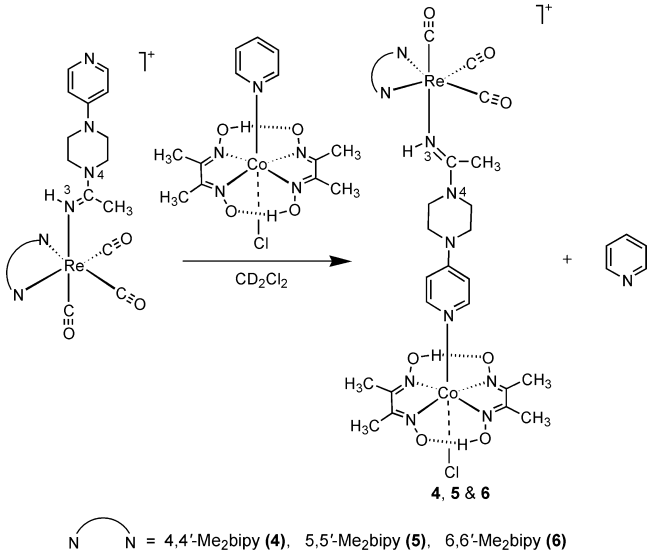

Re,Co dinuclear $[Re(CO)_3(Me_2bipy)(\mu\text{-}(HNC(CH_3)\text{-}(pyppz)))Co(DH)_2Cl]BF_4$ complexes (Me_2bipy = 4,4′-Me_2bipy (**4**), 5,5′-Me_2bipy (**5**), and 6,6′-Me_2bipy (**6**)) in 65−80% yields. ^1H NMR spectroscopic data (Table 1, see also Supporting Information) and structural characterization by single-crystal X-ray crystallography show that the new mononuclear and dinuclear amidine complexes all contain only one detectable isomer, with the amidine in the *E* configuration (Figure 1), consistent with previous findings on related compounds.[4]

Structural Results. Overall Aspects. The crystal data and details of the structural refinement for complexes **2**, **3**, **5**, and **6** are summarized in Table 2. The ORTEP plots of the cations of **2**, **3**, **5**, and **6** are shown in Figures 3 and 4, along with the numbering scheme used to describe the solid-state data. Selected bond lengths and bond angles are presented in Table 3. In all complexes studied, the Re atom has a pseudo-octahedral geometry, with the three carbonyl ligands coordinated facially. The Re coordination sphere is completed by two nitrogen atoms of the bidentate Me_2bipy ligand and by one nitrogen atom (N3) of the neutral monodentate amidine ligand (Figures 3 and 4). For the purposes of this discussion, the coordination plane defined by Re, Me_2bipy, and the two CO groups trans to Me_2bipy will be called the equatorial plane; the other CO and the amidine ligand in the complex are referred to as axial ligands. The Re−C bond distances for the axial and equatorial CO ligands (Figures 3 and 4) are generally not significantly different. This finding is consistent with structural data reported for recently synthesized amidine complexes of the type $[Re(CO)_3(Me_2bipy)(HNC(CH_3)N\text{-}(CH_2CH_2)_2Y)]BF_4$.[4] In the Re,Co binuclear complexes **5** and **6**, the cobalt center has a distorted octahedral geometry, with the four equatorial positions occupied by the nitrogen donor atoms of the two monoanionic DH ligands. The axial positions are occupied by Cl and the pyridyl N of the pyppz moiety of the amidine ligand.

Structural Features of the Me_2Bipy Equatorial Ligand. The tilting of the plane of the 6,6′-Me_2bipy ligand out of the equatorial coordination plane in **3** and **6** (Figure 5 and Supporting Information, Figure S1) is expected,[4,19,20] because otherwise the methyl groups of the 6,6′-Me_2bipy ligand and the two equatorial CO ligands would clash. The tilting typically moves the methyl groups toward the axial CO.[4,19,20,54] As can be seen in Supporting Information, Figures S2 and S3, the 5,5′-Me_2bipy ligand in **2** is tilted in the same direction but less acutely than is the 6,6′-Me_2bipy ligand in **3** and **6**. In contrast, the 5,5′-Me_2bipy ligand in amidine complexes[4,19] normally is not tilted (Supporting Information, Figure S2). Furthermore, the 5,5′-Me_2bipy ligand is tilted in **5** also (Supporting Information, Figures S4 and S5), but in the direction opposite to that in **2**, **3**, and **6**. Despite the tilting, the Re−N bond lengths (in the equatorial plane) for **2**, **3**, **5**, and **6** (Table 3) are all comparable to typical Re−N (sp^2) bond lengths, which range from 2.15 to 2.21 Å.[4,19,55,56]

Amidine Ligand Structural Features and Relation to the Me_2Bipy Equatorial Ligand. The Re−N and C−N bond distances and the C−N−C and N−C−N bond angles (Table 3) all confirm that **2**, **3**, **5**, and **6** possess very similar rhenium-bound amidine ligands. The Re−N3 bond lengths (Table 3) showed no significant difference and are comparable to those of similar amidine and iminoether complexes.[4,19,20]

For **2**, **3**, **5**, and **6**, the C16−N bond lengths (Table 3) of the amidine ligand are all closer to the average sp^2 C═N bond length (∼1.28 Å) than to the average sp^3 C−N bond length (∼1.47 Å).[4,19] Also, the very slightly shorter C16−N3 bond distances indicate that the C16−N3 bond has more double-bond character than the C16−N4 bond.[4,19] The sp^2-like C16−N4−C18, C16−N4−C21, and N3−C16−N4 bond angles, all close to 120° (Table 3), confirm the electron delocalization within the amidine group.[4,19,20,57−59]

The orientation of the amidine ligand (specified by the projection of the amidine plane, defined by the N3, C16, and N4 atoms, onto the equatorial plane) is similar for **2**, **3**, and **6** (Figures 3 and 4). This orientation, with the two N−Re−C angles in the equatorial plane bisected by the plane of the amidine ligands, has also been found for other amidine complexes.[4,19] From **2**, **3**, **6**, and structures in previous studies,[4,19] we can conclude that this "normal" orientation of

dx.doi.org/10.1021/ic5016675 | Inorg. Chem. 2014, 53, 11096−11107

Table 2. Crystal Data and Structural Refinement for $[Re(CO)_3(Me_2bipy)(HNC(CH_3)(pyppz))]BF_4$ and $[Re(CO)_3(Me_2bipy)(\mu$-$(HNC(CH_3)(pyppz)))Co(DH)_2Cl]BF_4$ Complexes

	2 (5,5′-Me_2bipy)	**3** (6,6′-Me_2bipy)	**5** (5,5′-Me_2bipy)	**6** (6,6′-Me_2bipy)
empirical formula	$C_{26}H_{28}N_6O_3Re{\cdot}BF_4$	$C_{26}H_{28}N_6O_3Re{\cdot}BF_4$	$C_{34}H_{42}ClCoN_{10}O_7Re{\cdot}CH_2Cl_2{\cdot}BF_4$	$C_{34}H_{42}ClCoN_{10}O_7Re{\cdot}C_4H_{10}O{\cdot}BF_4$
fw	745.55	745.55	1155.09	1144.29
crystal system	monoclinic	monoclinic	orthorhombic	triclinic
space group	$P2_1/n$	$P2_1/n$	$P2_12_12_1$	$P\bar{1}$
a (Å)	8.6106(4)	8.8914(10)	14.963(2)	10.997(3)
b (Å)	31.9058(13)	26.195(3)	16.604(2)	14.686(3)
c (Å)	30.2319(13)	12.5039(15)	17.856(2)	16.078(4)
α				105.787(15)
β (deg)	93.653(2)	110.199(5)		105.748(15)
γ				102.678(14)
V (Å^3)	8288.7(6)	2733.2(5)	4436.2(9)	2281.1(10)
T (K)	90	90	90	90
Z	12	4	4	2
ρ_{calcd} (Mg/m^3)	1.792	1.812	1.729	1.666
abs. coeff. (mm^{-1})	9.20	4.51	3.36	3.15
θ_{max} (deg)	67.9	30.6	25.4	27.6
R [$I > 2\sigma(I)$][a]	0.041	0.025	0.036	0.050
wR^2[b]	0.113	0.053	0.075	0.122
data/parameters	14 122/1099	8368/377	7646/559	10 019/605
res. dens (e Å^{-3})	1.63, −1.27	2.12, −1.32	1.32, −1.02	3.49, −1.47

[a] $R = (\sum||Fo| - |Fc||)/\sum|Fo|$. [b] $wR^2 = [\sum w(Fo^2 - Fc^2)^2]/\sum w(Fo^2)^2]^{1/2}$, in which $w = 1/[\sigma^2(Fo^2) + (dP)^2 + (eP)]$ and $P = (Fo^2 + Fc^2)/3$.

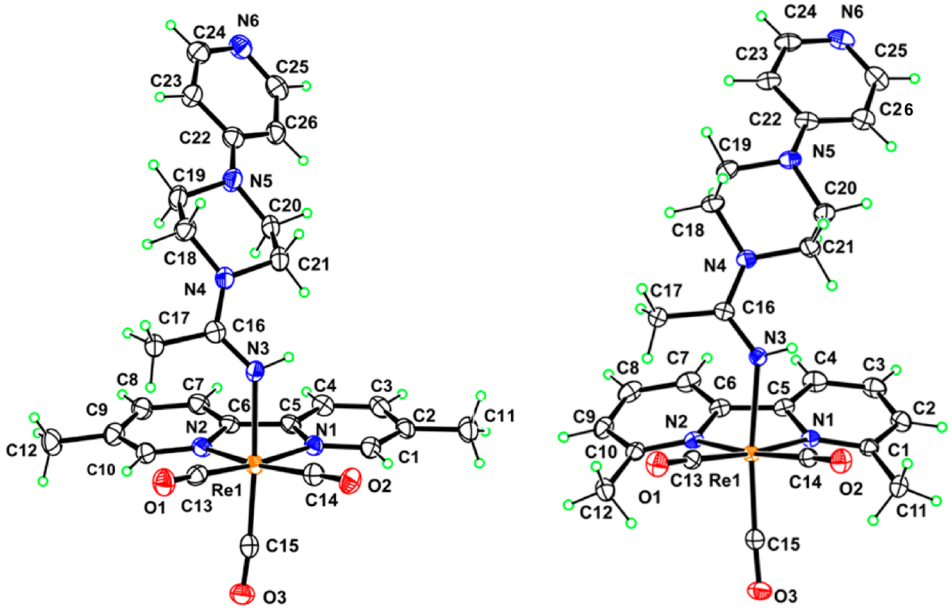

Figure 3. ORTEP plots of the cations of $[Re(CO)_3(5,5'\text{-}Me_2bipy)(HNC(CH_3)(pyppz))]BF_4$ (**2**) (left) and $[Re(CO)_3(6,6'\text{-}Me_2bipy)(HNC(CH_3)(pyppz))]BF_4$ (**3**) (right). Thermal ellipsoids are drawn with 50% probability.

the amidine ligand in the solid state is not very dependent on either the substitution pattern of the Me_2bipy ligand or the size and shape of the amidine ligand.[4,19] However, there are occasional exceptions, and the orientation of the amidine ligand in **5** (Figure 4) is one such exception. In **5** the plane of the amidine ligand bisects the C13−Re−C14 and N1−Re−N2 angles.

For **2**, **3**, and **6** (Figures 3 and 4), which have the normal amidine orientation, the bond angles from the equatorial N atoms to the axial N3 atom (N1−Re−N3 and N2−Re−N3) are statistically different (Table 3), as also observed in previous studies.[4,19,20] Previously the larger N−Re−N3 bond angle was thought to be caused by steric repulsion between the methyl group of the axial amidine[4,19] or axial iminoether[20] ligand and the closest atoms of the equatorial ligands. For example, we found for $[Re(CO)_3(Me_2bipy)(HNC(CH_3)N(CH_2CH_2)_2Y]$-$BF_4$ complexes[4] that the average of the larger of the two N−Re−N3 bond angles was greater in the 5,5′-Me_2bipy complexes than in the 6,6′-Me_2bipy complexes. Furthermore, the difference between the two angles was usually larger for the 5,5′-Me_2bipy complexes than for the 6,6′-Me_2bipy complexes.[4] The space near the axial amidine coordination site (trans to the axial CO) was assessed by using the nonbonded distances from N3 to the Me_2bipy carbon and nitrogen atoms.[4,20] It was concluded that the tilting of the 6,6′-Me_2bipy ligand results in a significant decrease in the interactions between the methyl group of the

dx.doi.org/10.1021/ic5016675 | Inorg. Chem. 2014, 53, 11096−11107

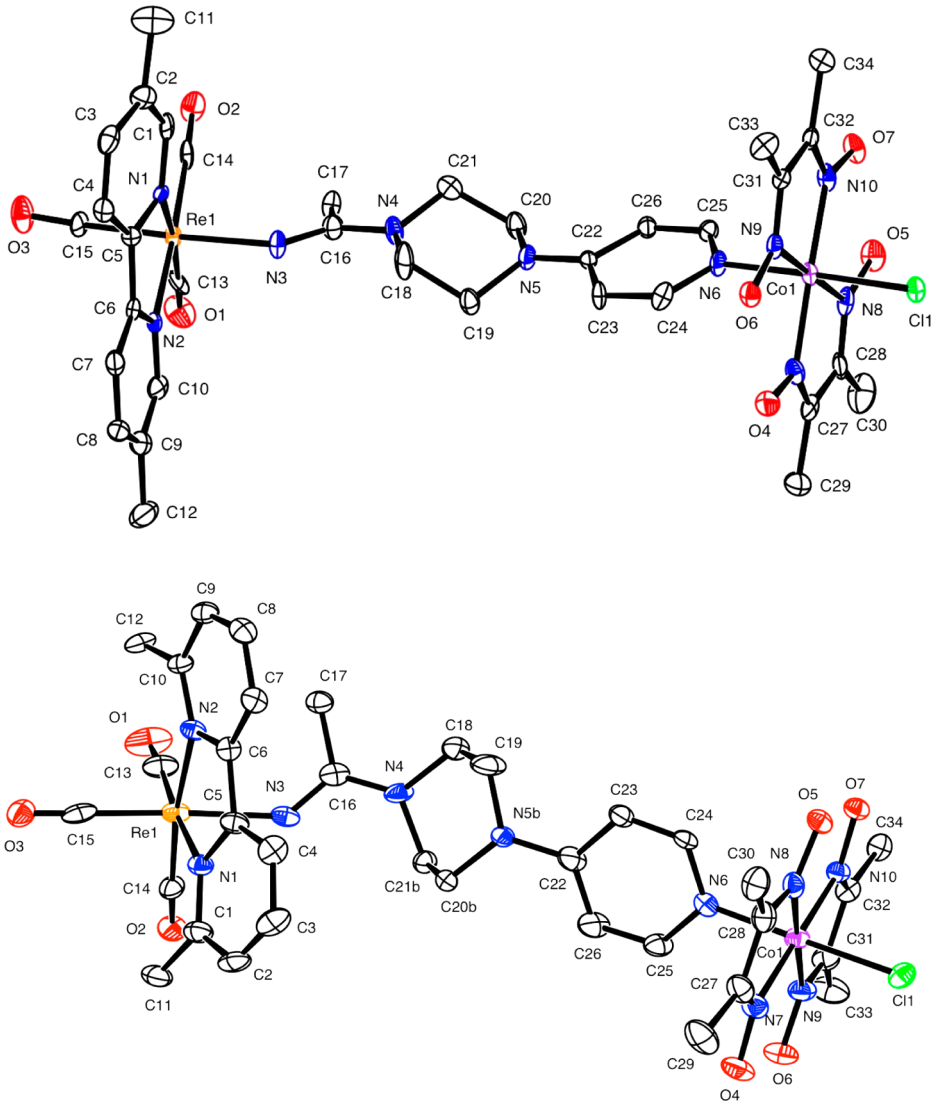

Figure 4. ORTEP plots of the cations of $[Re(CO)_3(5,5'\text{-}Me_2bipy)(\mu\text{-}(HNC(CH_3)(pyppz)))Co(DH)_2Cl]BF_4$ (**5**) (upper) and $[Re(CO)_3(6,6'\text{-}Me_2bipy)(\mu\text{-}(HNC(CH_3)(pyppz)))Co(DH)_2Cl]BF_4$ (**6**) (lower). Thermal ellipsoids are drawn with 50% probability.

axial iminoether or amidine ligand and the equatorial Me_2bipy ligand in the 6,6′-Me_2bipy complexes versus the 5,5′-Me_2bipy analogue.[4]

However, unlike previous findings,[4,19,20] the size of the larger of the two N−Re−N3 (N2−Re−N3) bond angles in the 6,6′-Me_2bipy complex (**3**) is greater than the larger corresponding N2−Re−N3 bond angle in the 5,5′-Me_2bipy complex (**2**) (Table 3). The difference between the two N−Re−N3 bond angles in **2**, while significant, is very small (∼1°). In **6**, however, the N2−Re−N3 bond angle is much larger (>4°) than the N1−Re−N3 angle (Table 3). The plane of the 6,6′-Me_2bipy ligand in **6** is tilted out of the equatorial plane as expected (Figure 5 and Supporting Information, Figure S1).

The differences in the relative sizes of the N3−Re−N angles found here compared to such differences found in previous studies led us to compare the space near the amidine ligand in **2**, **3**, **5**, and **6** to that present in related complexes.[4,20] In this method, the Me_2bipy ligand is viewed as having an interior or "front side" (atoms C1, N1, N2, C10) and an exterior or "back side" (atoms C3, C4, C7, C8), according to the numbering scheme in Figures 3 and 4. The front-side nonbonded distances from N3 to C1 or C10 have relatively small differences (Table 4).

The back-side nonbonded distances from N3 to C4 and C7 average ∼0.7 Å shorter in **6** than in **5**. These differences are somewhat greater than the respective ∼0.5 Å differences found for the close analogues $[Re(CO)_3(Me_2bipy)(HNC(CH_3)N(CH_2CH_2)_2NH)]BF_4$, in which the amidine was derived from piperazine (Supporting Information).[4] The larger differences are attributed to the unusual opposite-direction tilting of the 5,5′-Me_2bipy ligand in **5** (Supporting Information, Figure S4). This tilting increases the nonbonded distances. In contrast to these large differences between **6** and **5**, the "back-side" nonbonded distances from N3 to C4 and C7 average only ∼0.2 Å shorter in **3** than in **2**, a difference smaller than for the $[Re(CO)_3(Me_2bipy)(HNC(CH_3)N(CH_2CH_2)_2NH)]BF_4$ analogues. The smaller differences in nonbonded distances in **3** than in **2** (as compared to the analogues) are chiefly the result of the normal-direction tilting of the 5,5′-Me_2bipy ligand in **2** (Supporting Information, Figure S3). Such tilting is unusual for a 5,5′-Me_2bipy analogue.

We attribute the structural differences in this report as compared to those for previously studied Me_2bipy amidine

dx.doi.org/10.1021/ic5016675 | Inorg. Chem. 2014, 53, 11096−11107

Table 3. Selected Bond Distances (Å) and Angles (deg) for $[Re(CO)_3(Me_2bipy)(HNC(CH_3)(pyppz))]BF_4$ and $[Re(CO)_3(Me_2bipy)(\mu\text{-}(HNC(CH_3)(pyppz)))Co(DH)_2Cl]BF_4$ Complexes

	2 (5,5′-Me_2bipy)	3 (6,6′-Me_2bipy)	5 (5,5′-Me_2bipy)	6 (6,6′-Me_2bipy)
		bond distances		
Re−C13	1.933(5)	1.910(3)	1.902(7)	1.922(6)
Re−C14	1.935(6)	1.924(3)	1.914(8)	1.894(7)
Re−C15	1.922(6)	1.914(3)	1.905(6)	1.933(8)
Re−N1	2.185(4)	2.207(2)	2.169(5)	2.196(5)
Re−N2	2.179(5)	2.199(2)	2.168(6)	2.202(5)
Re−N3	2.177(5)	2.171(2)	2.165(5)	2.190(5)
C16−N3	1.310(7)	1.302(3)	1.291(8)	1.307(8)
C16−N4	1.344(7)	1.355(3)	1.352(8)	1.342(8)
Co−N6			1.946(5)	1.947(5)
Co−N7			1.891(6)	1.875(5)
Co−N8			1.896(6)	1.896(5)
Co−N9			1.885(6)	1.912(5)
Co−N10			1.876(6)	1.905(5)
Co−Cl			2.2391(18)	2.2272(17)
N7−O4			1.365(7)	1.344(7)
N8−O5			1.353(8)	1.322(7)
N9−O6			1.357(7)	1.325(7)
N10−O7			1.349(7)	1.356(6)
C27−N7			1.268(9)	1.292(8)
C28−N8			1.289(9)	1.306(8)
C31−N9			1.295(8)	1.302(8)
C32−N10			1.305(9)	1.293(7)
		bond angles		
N1−Re−N2	75.01(17)	74.51(8)	74.30(19)	75.90(18)
N1−Re−N3	79.49(17)	78.61(8)	82.90(2)	78.87 (18)
N2−Re−N3	81.06(16)	84.45(8)	86.2(2)	84.42 (18)
N3−Re−C13	95.8(2)	96.55(10)	98.7(3)	98.0 (3)
N3−Re− C14	94.7(2)	89.81(8)	93.9(3)	89.1(2)
Re−N3−H3N	113(5)	108(2)	120(5)	99(4)
Re−N3−C16	134.2(4)	137.71(19)	133.5(5)	137.4(5)
C16−N3−H3N	112(5)	112(2)	106(5)	123(4)
N3−C16−N4	123.3(5)	122.3(2)	124.1(6)	122.8(6)
N3−C16−C17	120.2(5)	119.8(2)	119.5(6)	119.6(6)
N4−C16−C17	116.5(5)	117.8(2)	116.4(6)	117.5(6)
C16−N4−C18	123.6(5)	123.7(2)	121.5(6)	124.7(6)
C16−N4−C21	124.5(5)	122.5(2)	123.5(6)	126.9(7)
N6−Co−Cl			178.00(18)	177.32(15)
N7−C27−C29			124.3(8)	122.8(7)
N8−C28−C30			122.6(7)	123.4(7)
N9−C31−C33			123.8(7)	122.6(6)
N10−C32−C34			122.5(7)	124.4(6)

complexes[4] to the influence on solid-state packing by the elongated axial amidine ligands in this work. Because tilting can be assessed from the NMR data (see below), we can determine if this is indeed a solid-state effect.

The axial N6−Co−Cl bond angles in **5** and **6** and the Co−N and Co−Cl axial bond distances (Table 3) are very similar to those of $(py)Co(DH)_2Cl$.[60] There are no noteworthy structural differences between the $Co(DH)_2Cl$ moiety in $(py)Co(DH)_2Cl$ and in **5** and **6**.[60]

NMR Spectroscopy. Complexes were characterized by ^1H NMR spectroscopy in CD_2Cl_2 (**1**−**6**) and CD_3CN (**2**, **3**, **5**, and **6**) (Table 1 and Supporting Information). The ^1H NMR spectra of all of the new $[Re(CO)_3(Me_2bipy)(HNC(CH_3)(pyppz))]BF_4$ complexes indicate that only the *E* isomer is present in solution. ^1H NMR signals of the Me_2bipy ligand were assigned from the splitting pattern, the integration, and by comparison to unambiguous assignments reported for $[Re(CO)_3(Me_2bipy)(HNC(CH_3)N(CH_2CH_2)_2Y)]BF_4$ complexes.[4] The atom-numbering system used in this discussion is shown in Scheme 1.

$[Re(CO)_3(Me_2bipy)(HNC(CH_3)(pyppz))]BF_4$ Mononuclear Complexes. Selected ^1H NMR signals of complexes **1**−**3** in CD_2Cl_2 (Table 1) reveal that the $C_{am}CH_3$ signal of **3** (1.95 ppm) is more upfield (by ∼0.4 ppm) than that of **1** (2.37 ppm) and **2** (2.38 ppm); this finding is attributed to the anisotropic effect of the 6,6′-Me_2bipy aromatic rings.[4] The distance from the $C_{am}CH_3$ methyl carbon to the centroid of the closer bipyridine ring in **3** (3.4 Å) is significantly shorter than in **2** (4.0 Å). This shorter distance results from the tilting in the 6,6′-Me_2bipy ligand, which moves the back side of the 6,6′-Me_2bipy ring up toward the amidine ligand (Supporting Information, Figure S1). The bipyridine rings thus exert a

dx.doi.org/10.1021/ic5016675 | Inorg. Chem. 2014, 53, 11096−11107

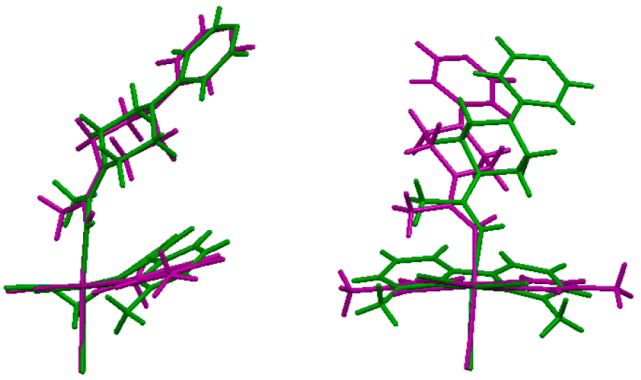

Figure 5. Overlay (root mean square = 0.137) of the Re and the O1, O2, and O3 atoms of the carbonyl ligands of $[Re(CO)_3(5,5'\text{-}Me_2bipy)(HNC(CH_3)(pyppz))]BF_4$ (**2**) (purple) and $[Re(CO)_3(6,6'\text{-}Me_2bipy)(HNC(CH_3)(pyppz))]BF_4$ (**3**) (green). The structures are depicted with the equatorial coordination plane perpendicular to the plane of the paper in a side view (left) and a front view (right) with the CO ligands toward the viewer.

greater anisotropic upfield-shifting effect on the $C_{am}CH_3$ signal for **3** than for **1** and **2**. As mentioned above, NMR shifts are sensitive to Me_2bipy tilting.[4] The shift of the $C_{am}CH_3$ signal for **2** is similar to that for **1**, indicating that the 5,5′-Me_2bipy ligand is not tilted in either complex. In addition, the shift for this signal for the related analogue $[Re(CO)_3(5,5'\text{-}Me_2bipy)(HNC(CH_3)N(CH_2CH_2)_2NH)]BF_4$, which has no tilted 5,5′-Me_2bipy ligand in the solid state, is at 2.12 ppm in CD_3CN.[4] For **2**, the shift in CD_3CN (Supporting Information, Table S2) is even slightly more downfield at 2.18 ppm, further establishing that the tilting in **2** (Supporting Information, Figure S2) is a solid-state effect.

The signal of the proton on the coordinated amidine N donor, N3H, is easily assigned because the peaks are broad singlets integrating to one proton. The signal is sensitive to tilt and also to the amidine substituent. The more downfield shift (~0.4 ppm) (Table 1) of the N3H signal of the 6,6′-Me_2bipy complex (**3**) than for complexes with other Me_2bipy isomers (**1** and **2**) is consistent with results for similar amidine complexes.[4] For **2** in CD_3CN, the N3H shift is 4.86 ppm (Supporting Information, Table S2), very similar to the corresponding shift (4.84 ppm) found for $[Re(CO)_3(5,5'\text{-}Me_2bipy)(HNC(CH_3)N(CH_2CH_2)_2NH)]BF_4$, with an untilted 5,5′-$Me_2bipy$ ligand.[4]

$[Re(CO)_3(Me_2bipy)(\mu\text{-}(HNC(CH_3)(pyppz)))Co(DH)_2Cl]BF_4$ Dinuclear Complexes. Except for the pyridyl ring signals (see below), the ^1H NMR signals of corresponding protons in both mononuclear and dinuclear complexes have similar shifts in both CD_2Cl_2 (Table 1) and CD_3CN (Supporting Information). Thus, spectra for **4**–**6** can be interpreted as discussed above for complexes **1**–**3**. In CD_2Cl_2, for example, the ~0.4 ppm more upfield $C_{am}CH_3$ signal of **6** versus those of **4** and **5** is a result of the anisotropic effect of the tilted 6,6′-Me_2bipy ligand in **6**, as discussed above for **3**.

The oxime CH_3 signals of complexes **4**–**6** all have the same shift, 2.31 ppm in CD_2Cl_2 (Table 1), a value very similar to that of $(py)Co(DH)_2Cl$ (2.35 ppm) (Supporting Information, Table S1). This finding is expected because shifts of the oxime CH_3 signals of cobaloximes ($LCo(DH)_2Cl$) are essentially independent of L when L is a planar N-donor heterocyclic aromatic ligand.[47] The O–H···O signals were easily assigned because they appeared farthest downfield as broad singlets integrating to two protons. The chemical shifts of the O–H···O signals for **4**–**6** (~18.4 ppm, Table 1) are very similar to that of $(py)Co(DH)_2Cl$ (18.37 ppm, Supporting Information, Table S1).

The shift changes ($\Delta\delta$) of the pyridyl ring H2/6 signals were upfield following the coordination of **1**, **2**, or **3** to form **4**, **5**, and **6** (Table 1). The upfield direction of $\Delta\delta$ for the H2/6 signals of $(py)Co(DH)_2$(monoanion) complexes is expected because it is known that the through-space shielding effect of the cobalt anisotropy on the signals of protons on the axial ligand closest to cobalt more than offsets the through-bond electron-withdrawing inductive deshielding effect of the positive metal ion.[41,47,61,62] The ~0.5–0.6 ppm $\Delta\delta$ values observed (Table 1) were larger than those typically found in $CDCl_3$.[41,47,61,62] However, the $\Delta\delta$ = 0.39 ppm observed upon $(py)Co(DH)_2Cl$ formation in CD_2Cl_2 (Supporting Information, Table S1) is relatively normal and similar to that found in $CDCl_3$ (0.34 ppm, Table 5). Thus, the only unusual NMR findings involved the H2/6 signals of the pyridyl group.

Effect of Basicity on the H2/6 ^1H NMR Signals of $LCo(DH)_2Cl$. To determine if the unusual effect on H2/6 $\Delta\delta$ values arises from the appended $[Re(CO)_3(Me_2bipy)(\mu\text{-}(HNC(CH_3)]$ moiety or from the basicity of the pendant pyridyl of **1**, **2**, and **3**, we examined the $\Delta\delta$ values of the H2/6 ^1H NMR signals for a series of $LCo(DH)_2Cl$ complexes, with L = a 4-substituted pyridine (4-Xpy). We employed 4-Xpy possessing varying electron-donating properties (estimated

Table 4. Selected Non-Bonded Distances (Å) for $[Re(CO)_3(Me_2bipy)(HNC(CH_3)(pyppz))]BF_4$ and $[Re(CO)_3(Me_2bipy)(\mu\text{-}(HNC(CH_3)(pyppz)))Co(DH)_2Cl]BF_4$ Complexes

	2 (5,5′-Me_2bipy)	**3** (6,6′-Me_2bipy)	**5** (5,5′-Me_2bipy)	**6** (6,6′-Me_2bipy)
N3–N1	2.789(6)	2.774(3)	2.870(9)	2.790(8)
N3–N2	2.831(6)	2.937(3)	2.962(8)	2.947(9)
C1–N3	3.628(7)	3.694(3)	3.602(9)	3.64(1)
C3–N3[a]	4.862(7)	4.647(4)	5.37(1)	4.64(1)
C4–N3[b]	4.259(7)	3.970(4)	4.901(9)	4.03(1)
C7–N3[b]	4.237(7)	4.084(5)	4.827(9)	4.28(1)
C8–N3[a]	4.880(7)	4.875(4)	5.33(1)	5.00(1)
C10–N3	3.709(7)	3.957(3)	3.696(9)	3.928(9)

[a]There is a small difference in these distances (average = 0.1 Å) for **2** and **3**, but for the analogues derived from piperazine the differences average ~0.3 Å.[4] For **5** and **6**, the differences average 0.5 Å. [b]Differences in these distances for **2** and **3** average ~0.2 Å, but for the analogues derived from piperazine this difference is ~0.45 Å.[4] For **5** and **6**, the differences average 0.7 Å.

dx.doi.org/10.1021/ic5016675 | Inorg. Chem. 2014, 53, 11096–11107

Table 5. pK_a and H2/6 NMR Shift (δ, ppm) of py and 4-Xpy Ligands in $CDCl_3$ at 25 °C. Changes in H2/6 Shift ($\Delta\delta$) on Formation of (py)Co(DH)$_2$Cl and (4-Xpy)Co(DH)$_2$Cl Complexes

L	pK_a[a]	L H2/6 δ	LCo(DH)$_2$Cl H2/6 δ	H2/6 $\Delta\delta$
4-CNpy	2.10[68]	8.82	8.54	0.28
py	5.25[69]	8.61	8.27	0.34
4-Mepy	5.98[70]	8.47	8.06	0.41
4-MeOpy	6.47[71]	8.43	8.00	0.43
4-$(CH_2)_5$Npy	9.6[b]	8.23	7.58	0.65
4-Me_2Npy	9.61[72]	8.22	7.63	0.59

[a] pK_a value obtained from refs 68–72. [b] Estimated.

from basicity as reflected in pK_a values) and chose the solvent used widely for NMR studies of cobaloximes, $CDCl_3$.[49,63–67] With increasing basicity of the free 4-Xpy ligands (4-CNpy < 4-Mepy < 4-MeOpy < 4-$(CH_2)_5$Npy ≈ 4-Me_2Npy), the shifts of the H2/6 signal were observed to be more upfield for both the ligand and its complex (Table 5). A linear plot for the shift dependence on basicity of the H2/6 signal of the (4-Xpy)Co(DH)$_2$Cl complexes has a steeper slope than the corresponding slope for the free ligand (Figure 6). Thus, the

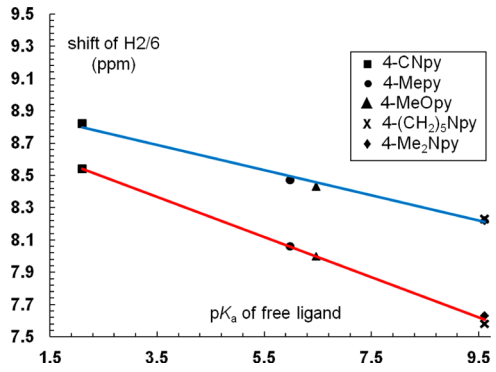

Figure 6. Plot of shift (ppm) of the H2/6 NMR signals of 4-Xpy ligands both free (blue line) and coordinated (red line) in (4-Xpy)Co(DH)$_2$Cl vs the pK_a value of the free ligands. The values for free 4-$(CH_2)_5$Npy and 4-Me_2Npy overlap.

$\Delta\delta$ values (0.28–0.65 ppm) correlate nonlinearly with the electron-donating properties of the pyridine ligands (Figure 7). [Figures 6 and 7 do not contain data for free py and

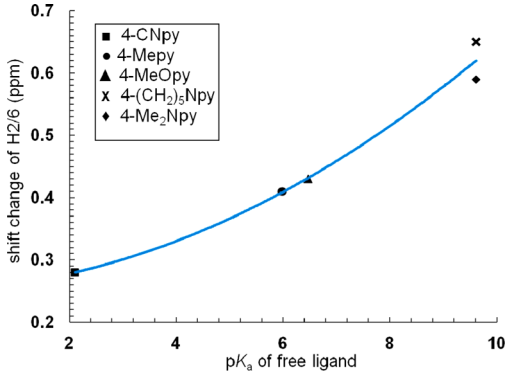

Figure 7. Plot of $\Delta\delta$ (ppm) [H2/6 NMR shift of free 4-Xpy ligand minus the shift of the corresponding ligand in (4-Xpy)Co(DH)$_2$Cl] vs the pK_a value of the ligand.

(py)Co(DH)$_2$Cl. These points lie off the lines shown, most likely because of the absence of a substituent at the 4 position. Inclusion of the points causes only slight differences in both the slopes and correlation coefficients, see Supporting Information.]

In conclusion, the large $\Delta\delta$ values for the H2/6 signal accompanying the coordination of **1**, **2**, and **3** to form **4**, **5**, and **6** are consistent with the expected strong electron-donating properties of **1**, **2**, and **3** as ligands, and the appended Re moiety does not exert any unusual effect.

Robustness of the Co–N Bond in the Dinuclear Complex, [Re(CO)$_3$(5,5′-Me$_2$bipy)(μ-(HNC(CH$_3$)(pyppz)))-Co(DH)$_2$Cl]BF$_4$ (5). A 5 mM solution of (4-Me_2Npy)Co(DH)$_2$Cl was treated with a molar equivalent of [Re(CO)$_3$(5,5′-Me$_2$bipy)(HNC(CH$_3$)(pyppz))]BF$_4$ (**2**), and the exchange reaction to form [Re(CO)$_3$(5,5′-Me$_2$bipy)(μ-(HNC(CH$_3$)(pyppz)))Co(DH)$_2$Cl]BF$_4$ (**5**) was monitored by ^{1}H NMR spectroscopy in $CDCl_3$. Small ^{1}H NMR signals corresponding to the "free" 4-Me_2Npy ligand and to **5** were detectable after 30 min. The intensity of these new signals gradually increased with time as the intensity of signals of (4-Me_2Npy)Co(DH)$_2$Cl and **2** decreased (Figure 8 and

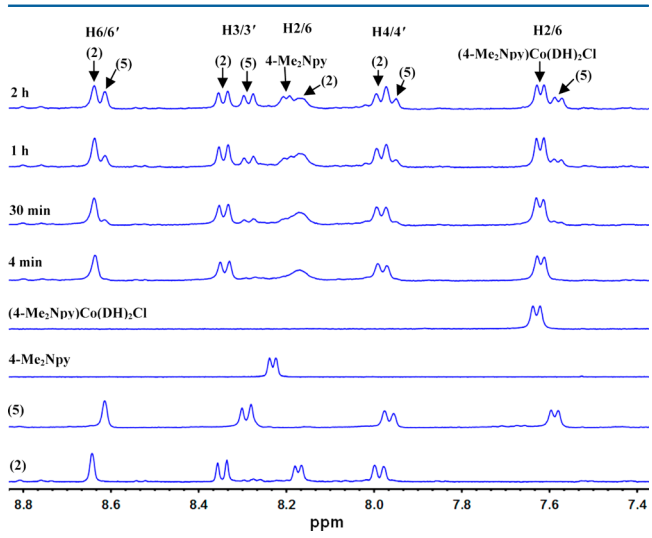

Figure 8. Aromatic ^{1}H NMR signals (in $CDCl_3$, 25 °C) for the exchange reaction of a 5 mM solution of (4-Me_2Npy)Co(DH)$_2$Cl with a molar equivalent of [Re(CO)$_3$(5,5′-Me$_2$bipy)(HNC(CH$_3$)(pyppz))]BF$_4$ (**2**) to form [Re(CO)$_3$(5,5′-Me$_2$bipy)(μ-(HNC(CH$_3$)(pyppz)))Co(DH)$_2$Cl]BF$_4$ (**5**) and free 4-Me_2Npy. More complete traces are shown in Supporting Information, Figure S8, which includes a 24 h spectrum essentially identical to the 2 h spectrum shown here.

Supporting Information, Figure S8). The intensities of the H2/6 and H3/5 signals of (4-Me_2Npy)Co(DH)$_2$Cl were approximately twice as large as for **5** at 24 h, indicating that the 4-Me_2Npy ligand is about twice as strong a donor as **2**.

We also examined the exchange reaction between [Re(CO)$_3$(5,5′-Me$_2$bipy)(μ-(HNC(CH$_3$)(pyppz)))Co(DH)$_2$Cl]BF$_4$ (**5**) and 4-Me_2Npy to form (4-Me_2Npy)Co(DH)$_2$Cl in $CDCl_3$. When a 5 mM solution was monitored by ^{1}H NMR spectroscopy, new ^{1}H NMR signals corresponding to both (4-Me_2Npy)Co(DH)$_2$Cl and "free" **2** were immediately observed. Because there were no significant differences between the first (~5 min) and last (24 h) ^{1}H NMR spectra recorded, we assumed that the exchange reaction was complete before the first spectrum was recorded. As shown in Figure 9 (see also

dx.doi.org/10.1021/ic5016675 | Inorg. Chem. 2014, 53, 11096–11107

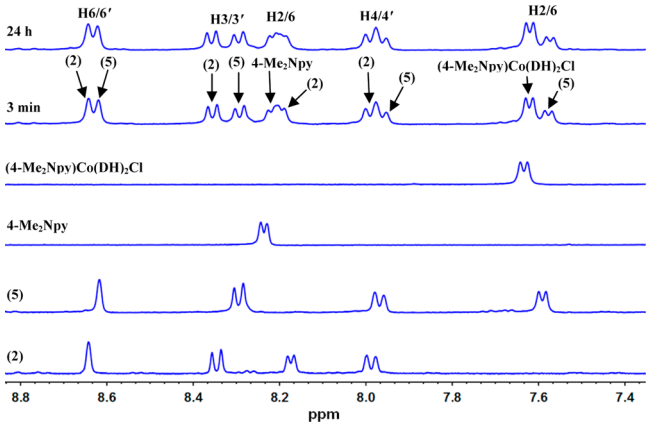

Figure 9. Aromatic region of ^{1}H NMR spectra (in $CDCl_3$, 25 °C) for the exchange reaction of a 5 mM solution of $[Re(CO)_3(5,5'\text{-}Me_2bipy)(\mu\text{-}(HNC(CH_3)(pyppz)))Co(DH)_2Cl]BF_4$ (**5**) with a molar equivalent of 4-Me_2Npy to form (4-Me_2Npy)$Co(DH)_2Cl$ and free $[Re(CO)_3(5,5'\text{-}Me_2bipy)(HNC(CH_3)(pyppz))]BF_4$ (**2**). More complete traces are shown in Supporting Information, Figure S9.

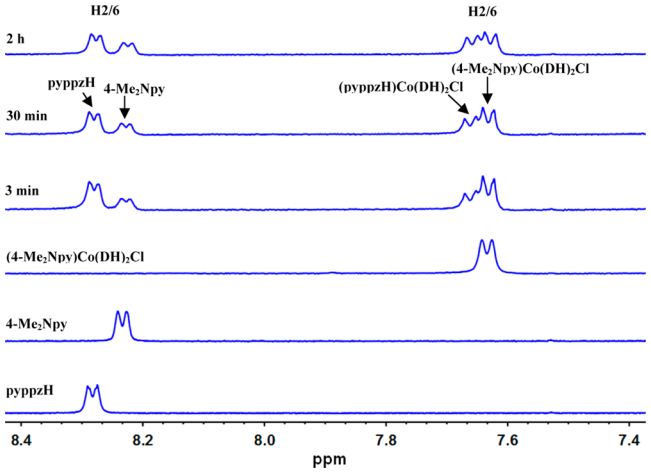

Figure 10. Aromatic ^{1}H NMR signals (in $CDCl_3$, 25 °C) for the exchange reaction of a 5 mM solution of (4-Me_2Npy)$Co(DH)_2Cl$ with a molar equivalent of pyppzH to form (pyppzH)$Co(DH)_2Cl$ and free 4-Me_2Npy. More complete traces are shown in Supporting Information, Figure S10, which includes spectra recorded at 1 h and at 24 h, both essentially identical to the 2 h spectrum shown here.

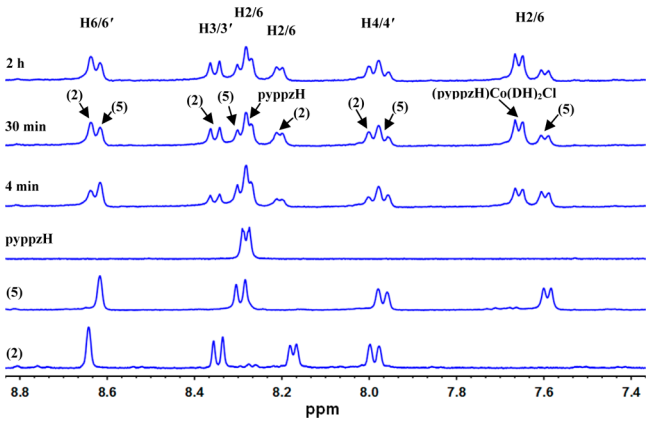

Figure 11. Aromatic ^{1}H NMR signals (in $CDCl_3$, 25 °C) for the exchange reaction of a 5 mM solution of $[Re(CO)_3(5,5'\text{-}Me_2bipy)(\mu\text{-}(HNC(CH_3)(pyppz)))Co(DH)_2Cl]BF_4$ (**5**) with a molar equivalent of pyppzH to form (pyppzH)$Co(DH)_2Cl$ and $[Re(CO)_3(5,5'\text{-}Me_2bipy)(HNC(CH_3)(pyppz))]BF_4$ (**2**). More complete traces are shown in Supporting Information, Figure S11, which includes spectra recorded at 1 h and at 24 h, both essentially identical to the 2 h spectrum shown here.

Supporting Information), the results are generally very similar to those obtained for the exchange reaction of (4-Me_2Npy)-$Co(DH)_2Cl$ and **2** and can thus confirm that 4-Me_2Npy is about twice as good a donor as **2**, consistent with **2** being a strong donor ligand.

To determine whether the appended $[Re(CO)_3(Me_2bipy)(\mu\text{-}(HNC(CH_3)]$ moiety in $[Re(CO)_3(5,5'\text{-}Me_2bipy)(HNC(CH_3)(pyppz))]BF_4$ (**2**) exerts an effect on the donor ability of the 4-pyridyl ring in pyppzH, we monitored by ^{1}H NMR spectroscopy the exchange reactions in $CDCl_3$ of pyppzH with (4-Me_2Npy)$Co(DH)_2Cl$ and also of pyppzH with $[Re(CO)_3(5,5'\text{-}Me_2bipy)(\mu\text{-}(HNC(CH_3)(pyppz)))Co(DH)_2Cl]BF_4$ (**5**). When a 5 mM solution of (4-Me_2Npy)$Co(DH)_2Cl$ was treated with a molar equivalent of pyppzH, small ^{1}H NMR signals corresponding to the free 4-Me_2Npy ligand and (pyppzH)$Co(DH)_2Cl$ were observed immediately. The intensity of these new signals gradually increased but remained constant after 1 h (Figure 10, see also Supporting Information). The intensities of the H2/6 and H3/5 signals of (4-Me_2Npy)$Co(DH)_2Cl$ were slightly greater than those of (pyppzH)$Co(DH)_2Cl$ even after 24 h. These results indicate that 4-Me_2Npy and pyppzH have similar donor ability, although 4-Me_2Npy is the slightly stronger donor. The exchange reaction between pyppzH and **5** to form (pyppzH)-$Co(DH)_2Cl$ was also monitored. New ^{1}H NMR signals corresponding to (pyppzH)$Co(DH)_2Cl$ and free **2** emerged immediately and grew gradually with time (Figure 11, see also Supporting Information). The intensities of the H2/6 and H3/5 signals of (pyppzH)$Co(DH)_2Cl$ were approximately twice as large as for **5** at 24 h, thus confirming that the pyppzH ligand is also about twice as good a donor as **2**. We can therefore conclude that the donor ability of the 4-pyridyl ring in pyppzH is lowered slightly when the proton on the nitrogen of the piperazine ring is replaced by the $Re(CO)_3(5,5'\text{-}Me_2bipy)$-$(HNC(CH_3)-$ moiety (in **2**).

CONCLUSIONS

All of the new $[Re(CO)_3(Me_2bipy)(HNC(CH_3)(pyppz))]BF_4$ and $[Re(CO)_3(Me_2bipy)(\mu\text{-}(HNC(CH_3)(pyppz)))Co(DH)_2Cl]BF_4$ complexes exist as only one isomer both in solution and in the solid state because steric interactions between the bulky $-C(CH_3)(pyppz)$ moiety of the axial amidine ligands and the equatorial Me_2bipy ligands highly favor the amidine ligand *E* configuration.

Mixtures of the B_{12} model (py)$Co(DH)_2Cl$ complex with $[Re(CO)_3(Me_2bipy)(HNC(CH_3)(pyppz))]BF_4$ complexes formed $[Re(CO)_3(Me_2bipy)(\mu\text{-}(HNC(CH_3)(pyppz)))Co(DH)_2Cl]BF_4$ complexes readily. The appended $[Re(CO)_3(Me_2bipy)(\mu\text{-}(HNC(CH_3)]$ moiety appears to cause only a slight lowering of the donor ability of the 4-pyridyl ring as compared to pyppzH. (The latter exhibits a donor ability very similar to that of the excellent 4-Me_2Npy donor ligand.) The findings of this study confirm that the amidine linkage can be used as a juncture for the conjugation of the *fac*-$[M^I(CO)_3]$ core (M = ^{99m}Tc and $^{186/188}$Re radionuclides) to biomedical targeting molecules such as B_{12} derivatives. Such a strategy may provide a successful method for the development of delivery

dx.doi.org/10.1021/ic5016675 | *Inorg. Chem.* 2014, 53, 11096−11107

systems for the targeted B_{12}-mediated delivery of radiopharmaceuticals.

The amidine ligands in the present work differ from those derived from heterocyclic amines studied previously[4] in that the second ring (pyridyl group) elongates the amidine, and this elongation is further increased by the $Co(DH)_2Cl$ moiety in the dinuclear complexes. We hypothesized that, in the solid state, packing forces distort structural features of the complex cations. For example, packing effects appear to counteract to some degree interligand repulsions in determining the relative sizes of the N−Re−N3 angles. In addition, in the solid state the 5,5′-Me_2bipy ligand is tilted in opposite directions in $[Re(CO)_3(5,5'\text{-}Me_2bipy)(HNC(CH_3)(pyppz))]BF_4$ (**2**) and $[Re(CO)_3(5,5'\text{-}Me_2bipy)(\mu\text{-}(HNC(CH_3)(pyppz)))Co(DH)_2Cl]BF_4$ (**5**), whereas no similar tilting was observed in previous studies.[4] This conclusion that solid-state effects influence the 5,5′-Me_2bipy ligand tilting and N−Re−N3 angle distortions is supported by NMR data.

In past studies, we found that the $C_{am}CH_3$ ^1H NMR signal is shifted upfield by the anisotropy of the tilted 6,6′-Me_2bipy ligand, but the $C_{am}CH_3$ ^1H NMR shift is similar within a given series of complexes, such as $[Re(CO)_3(5,5'\text{-}Me_2bipy)(HNC(CH_3)N(CH_2CH_2)_2Y)]BF_4$ or $[Re(CO)_3(6,6'\text{-}Me_2bipy)(HNC(CH_3)N(CH_2CH_2)_2Y)]BF_4$.[4,19,20,54] The shifts of the $C_{am}CH_3$ signals for **2**, **3**, **5**, and **6** in CD_3CN are very similar to those of the related analogues $[Re(CO)_3(5,5'\text{-}Me_2bipy)(HNC(CH_3)N(CH_2CH_2)_2NH)]BF_4$ and $[Re(CO)_3(6,6'\text{-}Me_2bipy)(HNC(CH_3)N(CH_2CH_2)_2NH)]BF_4$.[4] These analogues have undistorted solid-state structures. Thus, the NMR shifts confirm our conclusion that the elongated axial ligands of the new complexes reported here lead to the unusual angles and the 5,5′-Me_2bipy tilting found in the solid state.

■ ASSOCIATED CONTENT

Supporting Information

Crystallographic data for complexes **2**, **3**, **5**, and **6** in CIF format; ^1H NMR data for complexes **1**−**6** in CD_2Cl_2 (ppm); table of ^1H NMR chemical shifts of free py and of $(py)Co(DH)_2Cl$ in CD_2Cl_2; table of ^1H NMR chemical shifts of $[Re(CO)_3(Me_2bipy)(HNC(CH_3)(pyppz))]BF_4$ and $[Re(CO)_3(Me_2bipy)(\mu\text{-}(HNC(CH_3)(pyppz)))Co(DH)_2Cl]BF_4$ complexes in CD_3CN; tables comparing selected bond angles and nonbonded distances for **2** and **5** versus those of previously synthesized 5,5′-Me_2bipy complexes and for **3** and **6** versus those of previously synthesized 6,6′-Me_2bipy complexes; side views comparing **3** with **6**, and comparing **3** with **2**; overlay figures of the Re and the O1, O2, and O3 atoms of the carbonyl ligands comparing **2** with $[Re(CO)_3(5,5'\text{-}Me_2bipy)(HNC(CH_3)N(CH_2CH_2)_2CH_2)]BF_4$, comparing **2** with **5**, and comparing **5** with **6**; plots of shift of the H2/6 NMR signals of py and 4-Xpy both free and coordinated in cobaloximes, $(py)Co(DH)_2Cl$ and $(4\text{-}Xpy)Co(DH)_2Cl$, versus pK_a of free ligand; plot of $\Delta\delta$ (ppm) of the H2/6 NMR shift of free py and 4-Xpy ligand minus the shift of the corresponding ligand in $(py)Co(DH)_2Cl$ and $(4\text{-}Xpy)Co(DH)_2Cl$ versus the pK_a value of the ligand; ^1H NMR spectra ($CDCl_3$) of the exchange reactions of $(4\text{-}Me_2Npy)Co(DH)_2Cl$ with **2**, of 4-Me_2Npy with **5**, of pyppzH with $(4\text{-}Me_2Npy)Co(DH)_2Cl$, and of pyppzH with **5**. This material is available free of charge via the Internet at http://pubs.acs.org.

■ AUTHOR INFORMATION

Corresponding Author

*E-mail: lmarzil@lsu.edu.

Notes

The authors declare no competing financial interest.

■ ACKNOWLEDGMENTS

L.G.M. thanks Prof. Michael Threadgill, University of Bath, for useful discussions and the Raymond F. Schinazi International Exchange Programme between the University of Bath, UK and Emory University, Atlanta, USA for a Faculty Fellowship which provided support during the time that this research project was conceived.Upgrade of the diffractometer was made possible through Grant No. LEQSF(2011-12)-ENH-TR-01, administered by the Louisiana Board of Regents.

■ REFERENCES

(1) Schibli, R.; Schubiger, P. A. *Eur. J. Nucl. Med. Mol. Imaging* **2002**, *29*, 1529−1542.
(2) Desbouis, D.; Struthers, H.; Spiwok, V.; Kuster, T.; Schibli, R. *J. Med. Chem.* **2008**, *51*, 6689−6698.
(3) Abram, U.; Alberto, R. *J. Braz. Chem. Soc.* **2006**, *17*, 1486−1500.
(4) Abhayawardhana, P.; Marzilli, P. A.; Perera, T.; Fronczek, F. R.; Marzilli, L. G. *Inorg. Chem.* **2012**, *51*, 7271−7283.
(5) Perera, T.; Marzilli, P. A.; Fronczek, F. R.; Marzilli, L. G. *Inorg. Chem.* **2010**, *49*, 2123−2131.
(6) Lipowska, M.; Cini, R.; Tamasi, G.; Xu, X.; Taylor, A. T.; Marzilli, L. G. *Inorg. Chem.* **2004**, *43*, 7774−7783.
(7) Lipowska, M.; He, H.; Malveaux, E.; Xu, X.; Marzilli, L. G.; Taylor, A. *J. Nucl. Med.* **2006**, *47*, 1032−1040.
(8) Taylor, A. T.; Lipowska, M.; Marzilli, L. G. *J. Nucl. Med.* **2010**, *51*, 391−396.
(9) Alberto, R.; Schibli, R.; Abram, U.; Egli, A.; Knapp, F. F.; Schubiger, P. A. *Radiochim. Acta* **1997**, *79*, 99−103.
(10) Alberto, R.; Schibli, R.; Schubiger, A. P.; Abram, U.; Pietzsch, H. J.; Johannsen, B. *J. Am. Chem. Soc.* **1999**, *121*, 6076−6077.
(11) Murray, A.; Simms, M. S.; Scholfield, D. P.; Vincent, R. M.; Denton, G.; Bishop, M. C.; Price, M. R.; Perkins, A. C. *J. Nucl. Med.* **2001**, *42*, 726−732.
(12) Schibli, R.; Schwarzbach, R.; Alberto, R.; Ortner, K.; Schmalle, H.; Dumas, C.; Egli, A.; Schubiger, P. A. *Bioconjugate Chem.* **2002**, *13*, 750−756.
(13) Agorastos, N.; Borsig, L.; Renard, A.; Antoni, P.; Viola, G.; Spingler, B.; Kurz, P.; Alberto, R. *Chem.—Eur. J.* **2007**, *13*, 3842−3852.
(14) Cyr, J. E.; Pearson, D. A.; Wilson, D. M.; Nelson, C. A.; Guaraldi, M.; Azure, M. T.; Lister-James, J.; Dinkelborg, L. M.; Dean, R. T. *J. Med. Chem.* **2007**, *50*, 1354−1364.
(15) Bartholomä, M.; Valliant, J.; Maresca, K. P.; Babich, J.; Zubieta, J. *Chem. Commun.* **2009**, 493−512.
(16) Perera, T.; Abhayawardhana, P.; Marzilli, P. A.; Fronczek, F. R.; Marzilli, L. G. *Inorg. Chem.* **2013**, *52*, 2412−2421.
(17) He, H.; Lipowska, M.; Xu, X.; Taylor, A. T.; Marzilli, L. G. *Inorg. Chem.* **2007**, *46*, 3385−3394.
(18) He, H.; Lipowska, M.; Christoforou, A. M.; Marzilli, L. G.; Taylor, A. T. *Nucl. Med. Biol.* **2007**, *34*, 709−716.
(19) Perera, T.; Fronczek, F. R.; Marzilli, P. A.; Marzilli, L. G. *Inorg. Chem.* **2010**, *49*, 7035−7045.
(20) Perera, T.; Abhayawardhana, P.; Fronczek, F. R.; Marzilli, P. A.; Marzilli, L. G. *Eur. J. Inorg. Chem.* **2012**, 616−627.
(21) Lipowska, M.; He, H.; Xu, X.; Taylor, A. T.; Marzilli, P. A.; Marzilli, L. G. *Inorg. Chem.* **2010**, *49*, 3141−3151.
(22) Wei, L.; Babich, J. W.; Ouellette, W.; Zubieta, J. *Inorg. Chem.* **2006**, *45*, 3057−3066.
(23) Banerjee, S. R.; Levadala, M. K.; Lazarova, N.; Wei, L.; Valliant, J. F.; Stephenson, K. A.; Babich, J. W.; Maresca, K. P.; Zubieta, J. *Inorg. Chem.* **2002**, *41*, 6417−6425.

(24) Stephenson, K. A.; Zubieta, J.; Banerjee, S. R.; Levadala, M. K.; Taggart, L.; Ryan, L.; McFarlane, N.; Boreham, D. R.; Maresca, K. P.; Babich, J. W.; Valliant, J. F. *Bioconjugate Chem.* **2004**, *15*, 128−136.
(25) Russell-Jones, G.; McTavish, K.; McEwan, J.; Rice, J.; Nowotnik, D. *J. Inorg. Biochem.* **2004**, *98*, 1625−1633.
(26) Ruiz-Sanchez, P.; Mundwiler, S.; Medina-Molner, A.; Spingler, B.; Alberto, R. *J. Organomet. Chem.* **2007**, *692*, 1358−1362.
(27) Randaccio, L.; Geremia, S.; Demitri, N.; Wuerges, J. *Molecules* **2010**, *15*, 3228−3259.
(28) Viola-Villegas, N.; Rabideau, A. E.; Bartholoma, M.; Zubieta, J.; Doyle, R. P. *J. Med. Chem.* **2009**, *52*, 5253−5261.
(29) Waibel, R.; Treichler, H.; Schaefer, N. G.; van Staveren, D. R.; Mundwiler, S.; Kunze, S.; Kuenzi, M.; Alberto, R.; Nuesch, J.; Knuth, A.; Moch, H.; Schibli, R.; Schubiger, P. A. *Cancer Res.* **2008**, *68*, 2904−2911.
(30) Mahato, R.; Tai, W.; Cheng, K. *Adv. Drug Delivery Rev.* **2011**, *63*, 659−670.
(31) Mundwiler, S.; Spingler, B.; Kurz, P.; Kunze, S.; Alberto, R. *Chem.—Eur. J.* **2005**, *11*, 4089−4095.
(32) Ruiz-Sanchez, P.; Mundwiler, S.; Spingler, B.; Buan, N. R.; Escalante-Semerena, J. C.; Alberto, R. *J. Biol. Inorg. Chem.* **2008**, *13*, 335−347.
(33) Bagnato, J. D.; Eilers, A. L.; Horton, R. A.; Grissom, C. B. *J. Org. Chem.* **2004**, *69*, 8987−8996.
(34) Kunze, S.; Zobi, F.; Kurz, P.; Spingler, B.; Alberto, R. *Angew. Chem., Int. Ed.* **2004**, *43*, 5025−5029.
(35) Geremia, S.; Randaccio, L.; Marzilli, L. G. *Comprehensive Inorganic Chemistry II,* 2nd ed.; Elsevier: Amsterdam, 2013; Vol. *3*, pp 423−453.
(36) Spingler, B.; Mundwiler, S.; Ruiz-Sanchez, P.; van Staveren, D. R.; Alberto, R. *Eur. J. Inorg. Chem.* **2007**, 2641−2647.
(37) McGreevy, J. M.; Cannon, M. J.; Grissom, C. B. *J. Surg. Res.* **2003**, *111*, 38−44.
(38) Smeltzer, C. C.; Cannon, M. J.; Pinson, P. R.; Munger, J. D., Jr.; West, F. G.; Grissom, C. B. *Org. Lett.* **2001**, *3*, 799−801.
(39) Schmidt, S. P.; Trogler, W. C.; Basolo, F. *Inorg. Synth.* **1990**, *28*, 160−165.
(40) Edwards, D. A.; Marshalsea, J. *J. Organomet. Chem.* **1977**, *131*, 73−91.
(41) Trogler, W. C.; Stewart, R. C.; Epps, L. A.; Marzilli, L. G. *Inorg. Chem.* **1974**, *13*, 1564−1570.
(42) Sheldrick, G. M. *SADABS;* University of Göttingen: Germany, 1997.
(43) Sheldrick, G. M. *Acta Crystallogr., Sect. A: Found. Crystallogr.* **2008**, *A64*, 112−122.
(44) Trogler, W. C.; Epps, L. A.; Marzilli, L. G. *Inorg. Chem.* **1975**, *14*, 2748−2751.
(45) Schrauzer, G. N. *Acc. Chem. Res.* **1968**, *1*, 97−103.
(46) Brown, K. L.; Chernoff, D.; Keljo, D. J.; Kallen, R. G. *J. Am. Chem. Soc.* **1972**, *94*, 6697−6704.
(47) Bresciani-Pahor, N.; Forcolin, M.; Marzilli, L. G.; Randaccio, L.; Summers, M. F.; Toscano, P. J. *Coord. Chem. Rev.* **1985**, *63*, 1−125.
(48) Stewart, R. C.; Marzilli, L. G. *J. Am. Chem. Soc.* **1978**, *100*, 817−822.
(49) Toscano, P. J.; Marzilli, L. G. *Inorg. Chem.* **1979**, *18*, 421−424.
(50) Epps, L. A.; Marzilli, L. G. *J. Chem. Soc., Chem. Commun.* **1972**, 109−110.
(51) Marzilli, L. G.; Stewart, R. C.; Epps, L. A.; Allen, J. B. *J. Am. Chem. Soc.* **1973**, *95*, 5796−5798.
(52) Marzilli, L. G.; Salerno, J. G.; Epps, L. A. *Inorg. Chem.* **1972**, *11*, 2050−2053.
(53) Marzilli, L. G. *Inorg. Chem.* **1972**, *11*, 2504−2506.
(54) Liddle, B. J.; Lindeman, S. V.; Reger, D. L.; Gardinier, J. R. *Inorg. Chem.* **2007**, *46*, 8484−8486.
(55) He, H.; Lipowska, M.; Xu, X.; Taylor, A. T.; Carlone, M.; Marzilli, L. G. *Inorg. Chem.* **2005**, *44*, 5437−5446.
(56) Christoforou, A. M.; Fronczek, F. R.; Marzilli, P. A.; Marzilli, L. G. *Inorg. Chem.* **2007**, *46*, 6942−6949.
(57) Lefevre, X.; Durieux, G.; Lesturgez, S.; Zargarian, D. *J. Mol. Catal. A: Chem.* **2011**, *335*, 1−7.
(58) Rozenel, S. S.; Kerr, J. B.; Arnold, J. *Dalton Trans.* **2011**, *40*, 10397−10405.
(59) Cini, R.; Caputo, P. A.; Intini, F. P.; Natile, G. *Inorg. Chem.* **1995**, *34*, 1130−1137.
(60) Geremia, S.; Dreos, R.; Randaccio, L.; Tauzher, G.; Antolini, L. *Inorg. Chim. Acta* **1994**, *216*, 125−129.
(61) Marzilli, L. G.; Politzer, P.; Trogler, W. C.; Stewart, R. C. *Inorg. Chem.* **1975**, *14*, 2389−2393.
(62) Marzilli, L. G.; Gerli, A.; Calafat, A. M. *Inorg. Chem.* **1992**, *31*, 4617−4627.
(63) Bresciani-Pahor, N.; Randaccio, L.; Toscano, P. J. *J. Chem. Soc., Dalton Trans.* **1982**, 1559−1563.
(64) Stewart, R. C.; Marzilli, L. G. *Inorg. Chem.* **1977**, *16*, 424−427.
(65) Toscano, P. J.; Chiang, C. C.; Kistenmacher, T. J.; Marzilli, L. G. *Inorg. Chem.* **1981**, *20*, 1513−1519.
(66) Toscano, P. J.; Swider, T. F.; Marzilli, L. G.; Bresciani-Pahor, N.; Randaccio, L. *Inorg. Chem.* **1983**, *22*, 3416−3421.
(67) Randaccio, L.; Bresciani-Pahor, N.; Orbell, J. D.; Calligaris, M.; Summers, M. F.; Snyder, B.; Toscano, P. J.; Marzilli, L. G. *Organometallics* **1985**, *4*, 469−478.
(68) Stilinović, V.; Kaitner, B. *Cryst. Growth Des.* **2012**, *12*, 5763−5772.
(69) Linnell, R. *J. Org. Chem.* **1960**, *25*, 290−290.
(70) Scriven, E. F. V.; Murugan, R. *Kirk-Othmer Encyclopedia of Chemical Technology;* John Wiley & Sons, Inc.: Hoboken, NJ, 2006; Vol. *21*, pp 91−133.
(71) Dawson, R. M. C. *Data for Biochemical Research,* 3rd ed.; Oxford Science Publications: Clarendon, Oxford, 1986.
(72) Honda, H. *Molecules* **2013**, *18*, 4786−4802.